THE UNIVERSITY OF MICHIGAN

COLLEGE OF ENGINEERING

DEPARTMENT OF ELECTRICAL ENGINEERING

Radiation Laboratory

VOR PARASITIC LOOP COUNTERPOISE SYSTEMS - II

Interim Report No. 2 (1 November 1969 - 31 January 1970)

By
Dipak L. Sengupta and Joseph E. Ferris

15 February 1970

Contract FA 69-WA-2085, Project 330-001-03N

Contract Monitor: Mr. Sterling Anderson

CONTRACT WITH

Federal Aviation Administration
Radar and Navaids Section
800 Independence, SW
Washington, DC 20590

Ann Arbor, Michigan

1. Introduction

This is the Second Interim Report on Contract FA 69-WA-2085, Project 330-001-03N "VOR Parasitic Loop Counterpoise Systems-II" and covers the period 1 November 1969 to 31 January 1970.

During this period we have carried out some basic theoretical and experimental investigations of the radiation characteristics of parasitic loop counterpoise antennas having a figure-of-eight type of excitation in the azimuthal plane. As a result of this kind of excitation, the induced currents in the parasitic loops become non-uniform. The non-uniformity of the parasitic currents causes the optimum parameters (if any) and the performance of the antenna to be different than those obtained in the omnidirectionally excited antennas. The major effect of the non-uniform excitation has been found to give rise to a strong lobe in the axial direction of the far field pattern. The investigation reported herein has been undertaken in order to optimize the performance of the antenna under such situations.

The theoretical problems discussed in this report have the ultimate objective of developing complete theoretical expressions for the radiation field produced by non-uniformly excited parasitic loop counterpoise antennas. Experimental investigation has been confined to the case of non-uniformly excited double parasitic loop counterpoise antennas. Special emphasis has been given to obtain an optimum configuration for the 5.2' diameter counterpoise case.

2. Mutual Coupling Effects in Parasitic Loop Counterpoise Antennas

This section deals with the theoretical investigation of mutual coupling effects in a double parasitic loop counterpoise antenna. The theory of a single parasitic loop counterpoise antenna has been discussed elsewhere (Sengupta and Weston, 1969). In a previous report (Sengupta et al, 1968), an approximate theory was developed for the double parasitic loop counterpoise antenna by neglecting the effects of mutual coupling. There, the far field radiation pattern produced by the antenna was obtained by simply superposing individual free space fields. This theory explains with a fair amount of accuracy the far field for the cases when the spacing between the parasitic elements is large compared too widely spaced, the interaction betical situation where the loops are not to widely spaced, the interaction between the parasitic currents may become quite important. It is the purpose of this section to develop theoretical expressions for the parasitic currents and also for the far field produced by a double parasitic loop counterpoise antenna by taking into account the effects of mutual coupling.

2.1 Parasitic Currents

Consider a double parasitic loop counterpoise antenna as shown in Fig. 1.

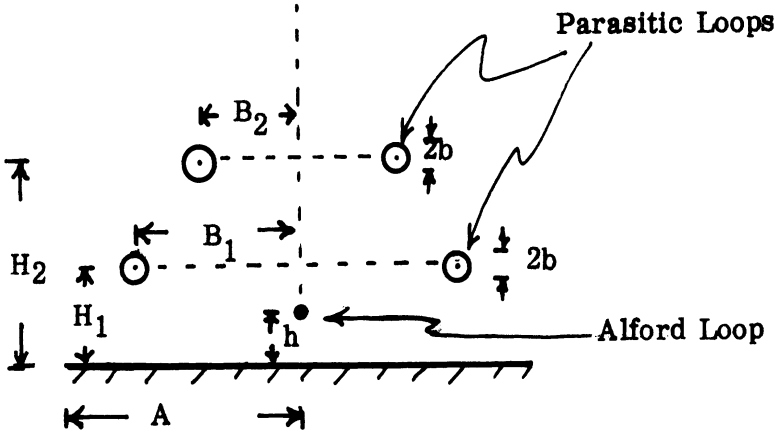

FIG. 1: Double Parasitic Loop Counterpoise Antenna.

The Alford loop situated at a height h above the counterpoise is the only excited element. Let I_1^T and I_2^T be the total currents in the two parasitic loops maintained by the excited element. Symmetry of the system and the nature of the excitation dictate that the distribution of the current along each parasitic element will be constant. Let us assume that in the absence of mutual coupling between the parasitic loops, the induced parasitic currents will be represented by I_1^O and I_2^O respectively. The method of determining I_1^O and I_2^O for the above configuration has been discussed elsewhere (Sengupta et al, 1968). By taking the mutual interaction into account we can write

$$I_1^T = I_2^O + K_{21} I_2^T \tag{1}$$

$$I_2^T = I_2^O + K_{12} I_1^T , \tag{2}$$

where K_{12} and K_{21} may be defined as the coefficients of coupling for the mutually induced currents.

Notice that these are not the conventional coefficients of mutual coupling and hence $K_{12} \neq K_{21}$. From (1) and (2) the following are obtained for the parasitic currents:

$$I_1^T = \frac{I_1^O + K_{21} I_2^O}{1-K_{21}K_{12}}, \tag{3}$$

$$I_2^T = \frac{I_2^O + K_{12} I_1^O}{1-K_{12}K_{21}} . \tag{4}$$

In general K_{12}, K_{21} are complex constants for a particular configuration of the antenna and $|K_{12}|$, $|K_{21}| < 1$. Thus the problem reduces to the determination of these two coefficients. We discuss this in the next section.

2.2 Determination of the Coupling Coefficients K_{12}, K_{21}

We outline here the basic mathematical setps involved in obtaining K_{12}. For this purpose we represent the antenna configuration as shown in Fig. 2.

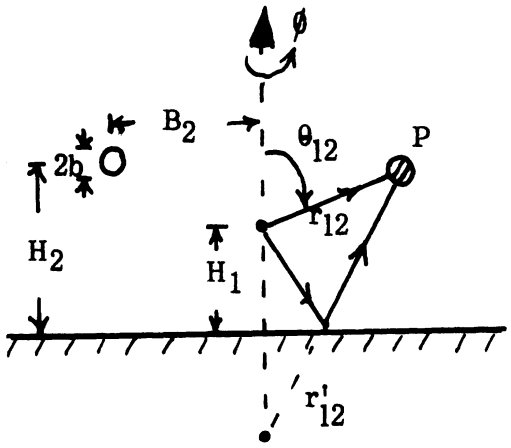

FIG. 2: Rays Contributing to K_{12}.

In this representation the first parasitic loop is replaced by a point source of suitable strength placed at a height H_1 above the counterpoise. The current in the first parasitic loop being I_1^T, the field produced by this current at the point P located on the second parasitic loop is given by:

$$E_\phi^{inc}(P) \simeq \eta_o I_1^T \left(\frac{kB_1}{2}\right)\left[J_1(kB_1\sin\theta_{12})\frac{e^{ikr_{12}}}{r_{12}} - J_1(kB_1\sin\theta'_{12})\frac{e^{ikr'_{12}}}{r'_{12}}\right], \quad (5)$$

where

η_o is the intrinsic impedance of free space,

$k = 2\pi/\lambda$ is the propagation constant in free space,

$$r_{12}^2 = B_2^2 + (H_2 - H_1)^2; \quad (r'_{12})^2 = B_2^2 + (H_2 + H_1)^2 \quad (6)$$

$$\sin\theta_{12} = \frac{B_2}{r_{12}}; \quad \sin\theta'_{12} = \frac{B_2}{r'_{12}} \quad . \quad (7)$$

J_1 is the Bessel function of the first kind and first order.

In Eq. (5) only the direct and the reflected fields due to the parasitic current I_1^T are used to obtain the incident field at P produced by this current; the contribution to the field at P due to diffraction effects at the edges of the counterpoise are neglected for the present. If necessary, they will be taken into account later. The current induced on the second parasitic loop due to the field $E_\phi^{inc}(P)$ is obtained by using the following relation.

$$I_2^{T'} \simeq \frac{2\pi}{i\eta_o kM} E_\phi^{inc}(P) , \quad (8)$$

where

$$M = 0.577 + \ell n\left(\frac{kb}{2}\right) - \frac{i\pi}{2} \quad . \quad (9)$$

After introducing Eq. (5) into (8) we obtain the following expression for K_{12}.

$$K_{12} = \frac{2\pi}{iM}\left(\frac{kB_1}{2}\right)\left[J_1(kB_1\sin\theta_{12})\frac{e^{ikr_{12}}}{kr_{12}} - J_1(kB_1\sin\theta'_{12})\frac{e^{ikr'_{12}}}{kr'_{12}}\right]. \quad (10)$$

Following a similar procedure it can be shown that the other coupling coefficient K_{21} is given by:

$$K_{21} = \frac{2\pi}{iM}\left(\frac{kB_2}{2}\right)\left[J_1(kB_2\sin\theta_{21})\frac{e^{ikr_{21}}}{kr_{21}} - J_1(kB_2\sin\theta'_{21})\frac{e^{ikr'_{21}}}{kr'_{21}}\right], \quad (11)$$

where

$$r_{21}^2 = B_1^2+(H_2-H_1)^2;\ (r'_{21})^2 = B_1^2+(H_2+H_1)^2, \quad (12)$$

$$\sin\theta_{21} = +\frac{B_1}{r_{21}};\ \sin\theta'_{21} = \frac{B_1}{r'_{21}}. \quad (13)$$

This completes the derivation of expressions for the coupling coefficients. In the next section we derive the explicit expressions for the parasitic currents due to the fields produced by the Alford loop carrying a current of magnitude I_o.

2.3 Expressions for the Parasitic Currents

It can be shown (Sengupta, et al 1968) that in the absence of mutual coupling the current induced in the first parasitic loop is given by

$$I_1^O = I_o\left(\frac{ka}{2}\right)^2\left[P_1+Q_1\right], \quad (14)$$

where a is the radius of the excited loop and,

$$P_1 = \frac{2\pi(kB_1)}{i\,M}\left[\frac{e^{ikr_1}}{(kr_1)^2} - \frac{e^{ikr_2}}{(kr_2)^2}\right] , \tag{15}$$

$$Q_1 = \frac{\pi^2(kB_1)}{M^2}\,\frac{e^{ikr_1}}{(kr_1)^2}\left[\left(\frac{1}{\pi kB_1}\right)^{1/2} e^{i(2kB_1+\pi/4)} - \left(\frac{1}{\pi kH_1}\right)^{1/2} e^{i(2kH_1-\pi/4)}\right], \tag{16}$$

$$r_1^2 = B_1^2 + (H_1-h)^2;\quad r_2^2 = B_1^2 + (H_1+h)^2 . \tag{17}$$

Similarly, the current induced in the second parasitic loop due to the field produced by the Alford loop only is given by the following:

$$I_2^O = I_o\left(\frac{ka}{2}\right)^2\left[P_2+Q_2\right] , \tag{18}$$

where

$$P_2 = \frac{2\pi\,(kB_2)}{iM}\left[\frac{e^{ikr_1'}}{(kr_1')^2} - \frac{e^{ikr_2'}}{(kr_2')^2}\right] , \tag{19}$$

$$Q_2 = \frac{\pi^2(kB_2)}{M^2}\,\frac{e^{ikr_1'}}{(kr_1')^2}\left[\left(\frac{1}{\pi kB_2}\right)^{1/2} e^{i(2kB_2+\pi/4)} - \left(\frac{1}{\pi kH_2}\right)^{1/2} e^{i(2kH_2-\pi/4)}\right], \tag{20}$$

$$(r_1')^2 = B_2^2 + (H_2-h)^2 ;\quad (r_2')^2 = B_2^2 + (H_2+h)^2 . \tag{21}$$

After using (3), (4), (10), (11) and (14) and (18), the parasitic currents I_1^T and I_2^T are obtained as follows:

$$I_1^T = I_o\left(\frac{ka}{2}\right)^2 \cdot \frac{1}{1-K_{12}K_{21}}\left[(P_1+Q_1)+K_{21}(P_2+Q_2)\right] \tag{22}$$

$$I_2^T = I_o\left(\frac{ka}{2}\right)^2 \frac{1}{1-K_{12}K_{21}}\left[(P_2+Q_2)+K_{12}(P_1+Q_1)\right] \quad . \tag{23}$$

Equations (22) and (23) are expressed so that they may be computed numerically. This would be done in the future. It should be noted that in the absence of mutual coupling, (22) and (23) reduce to (14) and (18) respectively.

2.4 Far Field Expressions

In this section the far field produced by the double parasitic loop counterpoise antenna will be given. The method of obtaining the expressions is similar to that discussed in the case of single parasitic loop counterpoise antennas (Sengupta and Weston, 1969) and hence will not be repeated here. All the expressions are arranged such that they may be programmed for numerical computation. The far field is expressed formally as:

$$E_\phi \sim \eta_o I_o \left(\frac{ka}{2}\right)^2 \frac{e^{i(kR-\pi/4)}}{R} \; S(\theta) \; , \tag{24}$$

where

$$S(\theta) = S^A(\theta) + S_1^P(\theta) + S_2^P(\theta) \; . \tag{25}$$

In the above equations $S(\theta)$ is identified with the complex far field pattern of the antenna; the three terms on the right hand side of (25) are the complex far field patterns produced by the Alford loop, the first and the second parasitic loops above the counterpoise. Explicit expressions for the three terms in (25) are given below for future reference.

$$S^A(\theta) = \left\{ \frac{F^o(\theta)\sin\theta}{\sqrt{2}} e^{-ikA\sin\theta} + \frac{|\cos\theta|\sin\left(\frac{\phi_o}{2}\right)}{\sqrt{\pi k r_o \sin\theta}} e^{ikr_o} L^o(\theta) \right\}, \tag{26}$$

$$L^{o}(\theta)=\frac{e^{i\left(\frac{\pi}{2}-kA\sin\theta\right)}}{\sqrt{1-\sin\theta}}\left[\frac{\cos^{3/2}\phi_o-\sin^{3/2}\theta}{\cos\phi_o-\sin\theta}\right]-\frac{e^{ikA\sin\theta}}{\sqrt{1+\sin\theta}}\left[\frac{\cos^{3/2}\phi_o}{\cos\phi_o+\sin\theta}\right], \tag{27}$$

$$F^{o}(\theta)=e^{ikr_o\sin(\theta-\phi_o)}\int_{-\infty}^{P_1} e^{i\pi t^2/2}\,dt-e^{ikr_o\sin(\theta+\phi_o)}\int_{-\infty}^{P_2} e^{i\pi t^2/2}\,dt, \tag{28}$$

$$P_1=2\left(\frac{kr_o}{\pi}\right)^{1/2}\cos\left(\frac{\phi_o-\theta-\pi/2}{2}\right), \tag{29}$$

$$P_2=2\left(\frac{kr_o}{\pi}\right)^{1/2}\cos\left(\frac{\phi_o-\theta-\pi/2}{2}\right), \tag{30}$$

$$r_o^2=A^2+h^2;\quad \tan\phi_o=\frac{h}{A}. \tag{31}$$

$$S_1^P(\theta)=\frac{kB_1}{2(1-K_{12}K_{21})}\left[(P_1+Q_1)+K_{21}(P_2+Q_2)\right]F_1(\theta), \tag{32}$$

where P_1, Q_1 are as given by Eqs. (15) and (16), and

$$F_1(\theta)=\frac{J_1(kB_1\sin\theta)}{\sqrt{2}}F_1^P(\theta)e^{-ikA\sin\theta}+\frac{|\cos\theta|\sin\left(\frac{\phi_{P_1}}{2}\right)}{\sqrt{\pi kr_{P_1}\sin\theta}}e^{ikr_{P_1}}L_1^P(\theta), \tag{33}$$

$$L_1^P(\theta)=\frac{e^{i\left(\frac{\pi}{2}-kA\sin\theta\right)}}{\sqrt{1-\sin\theta}}\left[\frac{\cos^{1/2}(\phi_{P_1})J_1(kB_1\cos\phi_{P_1})-\sin^{1/2}\theta J_1(kB_1\sin\theta)}{\cos\phi_{P_1}-\sin\theta}\right]$$
$$-\frac{e^{ikA\sin\theta}}{\sqrt{1+\sin\theta}}\left[\frac{J_1(kB_1\cos\phi_{P_1})\cos^{1/2}(\phi_{P_1})}{\cos\phi_{P_1}+\sin\theta}\right], \tag{34}$$

$$F_1^P(\theta) = e^{ikr_{P_1}\sin(\theta-\phi_{P_1})} \int_{-\infty}^{P_5} e^{i\pi t^2/2}\, dt$$

$$-e^{ikr_{P_1}\sin(\theta+\phi_{P_1})} \int_{-\infty}^{P_6} e^{i\pi t^2/2}\, dt\,, \tag{35}$$

$$P_5 = 2\left(\frac{kr_{P_1}}{\pi}\right)^{1/2} \cos\left(\frac{\phi_{P_1}-\theta-\pi/2}{2}\right)\,, \tag{36}$$

$$P_6 = 2\left(\frac{kr_{P_1}}{\pi}\right)^{1/2} \cos\left(\frac{\phi_{P_1}+\theta+\pi/2}{2}\right)\,, \tag{37}$$

$$r_{P_1}^2 = A^2 + H_1^2\,, \tag{38}$$

$$\tan\phi_{P_1} = H_1/A \tag{39}$$

$$S_2^P(\theta) = \frac{kB_2}{2(1-K_{12}K_{21})}\left[(P_2+Q_2+K_{12}(P_1+Q_1)\right] F_2(\theta) \tag{40}$$

where P_2, Q_2 are given by Eqs. (19) and (20),

$F_2(\theta)$ is given by Eqs. (33) - (39) with the parameters H_1, B_1 replaced by H_2 and B_2,

K_{12}, K_{21} are as given by Eqs. (10) and (11).

2.5 Discussion

Expressions for the parasitic currents and the far field produced by a double parasitic loop counterpoise antenna have been derived above by taking into account the dominent effects of mutual interaction between the parasitic elements. The relevant expressions for the induced currents and the far field are being computed at the present time. The results will be discussed in a future report.

3. The Radiation Field of a Circular Loop Carrying a Non-Uniform Current

3.1 Introduction

The radiation field produced by a circular loop carrying a non-uniform current is discussed theoretically in this section. The problem under investigation has direct bearing on the determination of the radiation field of a parasitic loop counterpoise antenna with a figure-of-eight type of excitation in the azimuthal plane. The non-uniform excitation causes the induced currents in the parasitic loops to be non-uniform. The performance of parasitic loop counterpoise antennas with non-uniform excitation cannot be explained by the theory developed for similar antennas with omnidirectional excitation. The present investigation is the first step toward the development of a theory for the non-uniformly excited parasitic loop counterpoise antenna.

3.2 Nature of Excitation

In a practical VOR antenna system, the figure-of-eight pattern in azimuth is obtained by placing two Alford loops side by side and exciting them with equal but out of phase signals. Let us consider two small circular loops (i.e. radius of the loop $<< \lambda$) carrying the currents of the form

$$I_o e^{-i\omega t} \quad \text{and} \quad I_o e^{-i(\omega t + \psi)}$$

be oriented along the x-axis as shown in Fig. 3.

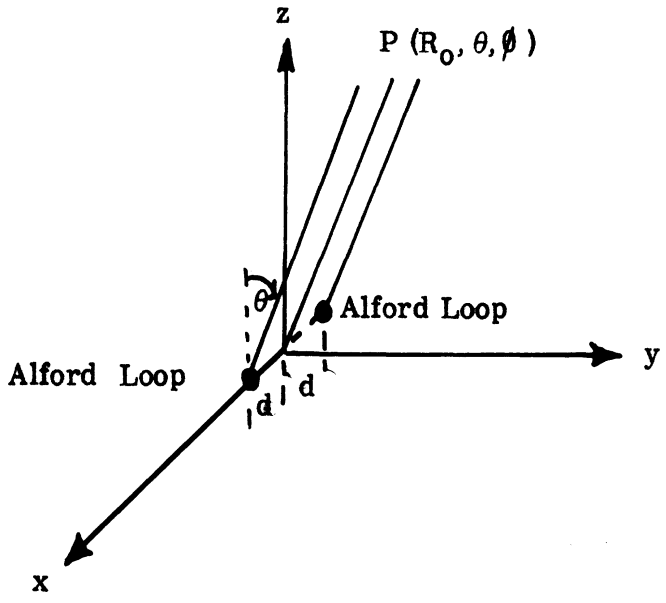

FIG. 3: Coordinate System Used.

The two loops lie in the xy plane. The two loops are separated by a distance 2d and the phase difference ψ between their currents is kept arbitrary for the present. It can be shown that the far field produced by the system at the point $P(R_o, \theta, \phi)$ is polarized in the ϕ-direction and is given by:

$$E_\phi = \eta_o I_o \left(\frac{ka}{2}\right)^2 \frac{e^{i(kR_o - \psi/2)}}{R_o} \, 2\sin\theta \cos\left[kd\sin\theta\cos\phi + \frac{\psi}{2}\right] \qquad (41)$$

where

η_o is the intrinsic impedance of free space,

$k = 2\pi/\lambda$ is the propagation constant in free space.

If $\psi = \pi$, then Eq. (41) reduces to the following

$$E_{\phi} = i2\eta_o I_o \left(\frac{ka}{2}\right)^2 \frac{e^{ikR_o}}{R_o} \sin\theta \sin\left[kd \sin\theta \cos\phi\right] . \qquad (42)$$

Eq. (42) indicates that in the azimuthal plane (θ = constant) the far field pattern is a figure-of-eight having maxima along $\phi = 0$ and π. Usually $kd \ll 1$ and under this assumption we can simplify (42) as follows:

$$E_{\phi} = i\, 2\eta_o \left(\frac{ka}{2}\right)^2 \frac{e^{ikR_o}}{R_o} (kd) \sin^2\theta \cos\phi . \qquad (43)$$

Any parasitic loop, placed with its axis along the z-axis will carry an induced current proportional to the field given by (43) or (42) as the case may be. To simplify our analysis we assume that the parasitic current in the present case is of the following form:

$$I = I_o \cos\phi , \qquad (44)$$

where I_o is a constant and ϕ is measured around the loop, the origin being at the x-axis. Equation (44) physically means that $I(\phi)$ vanishes at $\phi = \pm \pi/2$, where it reverses direction, so that the currents in the range

$$-\frac{\pi}{2} \leq \phi \leq \frac{\pi}{2}$$

are always counterclockwise when the currents in the range

$$\frac{\pi}{2} \leq \phi \leq \frac{3\pi}{2}$$

are clockwise. This may be looked upon as a dipole mode such that the charge density on the loop is $q(\phi) \alpha \sin\phi$. This means that the loop is oppositely charged at $\phi = \pi/2$ and $\phi = -\pi/2$ and the current oscillates in synchronism on the two halves much as in two parallel dipoles that are driven in phase. Notice that this is true regardless of the fact whether the parasitic loop is large or small.

3.3 Far Field Expressions

In this section we obtain the far field produced by a circular loop carrying a current of the form given by Eq. (44). The loop is oriented in the x-y plane as shown in Fig. 4.

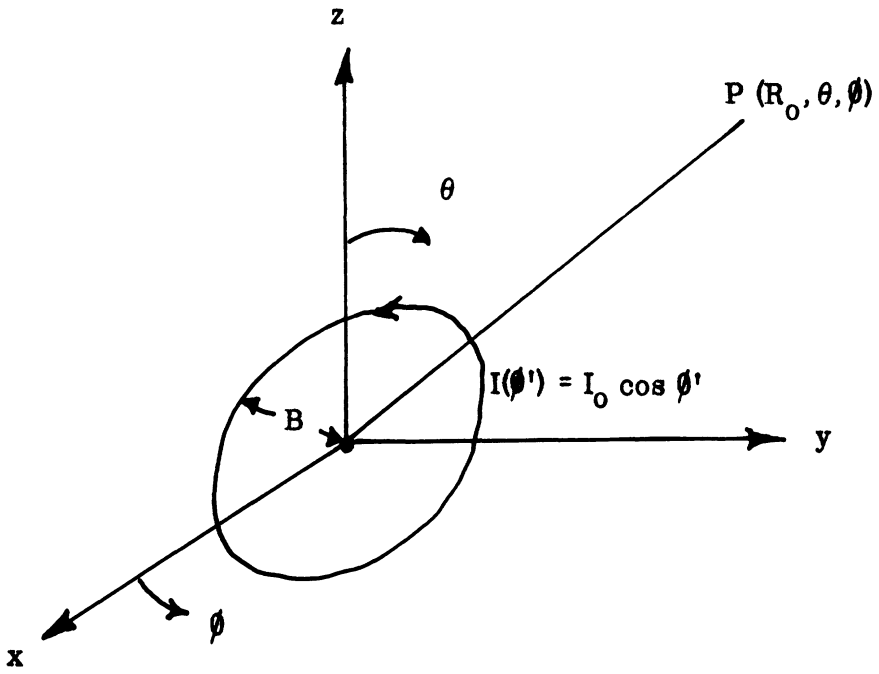

FIG. 4: Orientation of the Circular Loop.

To obtain the far field it is convenient to determine the vector potential $\bar{A}$ produced by the current at the far field point $P(R_o, \theta, \phi)$ and then obtain the field from the potential. With time dependence $e^{-i\omega t}$ and using standard notation the following expressions define the relationships between the fields and the vector potential:

$$\bar{E} = -i\omega \hat{r}_o \times (\hat{r}_o \times \bar{A}) = i\omega \left[\hat{\theta} A_\theta + \hat{\phi} A_\phi\right] , \tag{45}$$

$$\bar{B} = ik (\hat{r}_1 \times \bar{A}) = ik \left[\hat{\phi} A_\theta - \hat{\theta} A_\phi\right] , \tag{46}$$

where $\hat{r}_o$, $\hat{\theta}$, $\hat{\phi}$ are the unit vectors in R_o, θ and ϕ directions respectively. The components A_θ, A_ϕ of the vector potential in terms of the rectangular components are:

$$A_\theta = \left[A_x \cos\phi + A_y \sin\phi\right] \cos\theta, \tag{47}$$

$$A_\phi = -A_x \sin\phi + A_y \cos\phi \quad . \tag{48}$$

In the present configuration, as shown in Fig. 4, A_x and A_y are given by the following:

$$A_x = -\frac{\mu_o B}{4\pi} \frac{e^{ikR_o}}{R_o} \int_0^{2\pi} I(\phi') e^{-ikB\sin\theta\cos(\phi-\phi')} \sin\phi' \, d\phi' \tag{49}$$

$$A_y = \frac{\mu_o B}{4\pi} \frac{e^{ikR_o}}{R_o} \int_0^{2\pi} I(\phi') \, e^{-ikB\sin\theta\cos(\phi-\phi')} \cos\phi' \, d\phi' \tag{50}$$

where μ_o is the permeability of free space. After introducing (44) into (49) and (50) the following two equations are obtained:

$$A_x = -\frac{\mu_o B I_o}{8\pi} \frac{e^{ikR_o}}{R_o} \int_0^{2\pi} e^{-ikB \sin\theta\cos(\phi-\phi')} \sin 2\phi' \, d\phi' \, , \tag{51}$$

$$A_y = \frac{\mu_o B I_o}{8\pi} \frac{e^{ikR_o}}{R_o} \int_0^{2\pi} e^{-ikB\sin\theta\cos(\phi-\phi')} \, (1+\cos 2\phi') d\phi' \, . \tag{52}$$

To evaluate the integrals in (51) and (52) we make use of the following result:

$$\int_0^{2\pi} e^{i(n\pm 1)\phi'} e^{ikB\sin\theta\cos(\phi-\phi')} d\phi'$$

$$= 2\pi \, i^{n\pm 1} \, e^{i(n\pm 1)\phi} \, J_{n\pm 1}(kB\sin\theta) \, , \tag{53}$$

where $J_{n\pm 1}$ is the standard notation for the Bessel function of the first kind.

Using (53), we obtain the following from (51) and (52):

$$A_x = \frac{\mu_o B I_o}{4} \frac{e^{ikR_o}}{R_o} J_2(kB\sin\theta)\sin 2\phi \ , \tag{54}$$

$$A_y = \frac{\mu_o B I_o}{4} \frac{e^{ikR_o}}{R_o} \left[J_0(kB\sin\theta) - J_2(kB\sin\theta)\cos 2\phi\right] . \tag{55}$$

After introducing (54) and (55) into (47) and (48) and with some algebraic manipulation, we obtain

$$A_\theta = \frac{\mu_o B I_o}{2} \frac{e^{ikR_o}}{R_o} \frac{J_1(KB\sin\theta)}{(kB\sin\theta)} \cos\theta \sin\phi \ , \tag{56}$$

$$A_\phi = \frac{\mu_o B I_o}{2} \frac{e^{ikR_o}}{R_o} J_1'(kB\sin\theta) \cos\phi, \tag{57}$$

where the prime in Eq. (57) indicates differentiation with respect to the argument.

Using Eq.(45) along with Eqs. (56) and (57), we obtain the two components of the electric field in the far zone as given by the following:

$$E_\theta = i\eta_o I_o \left(\frac{kB}{2}\right) \frac{e^{ikR_o}}{R_o} \frac{J_1(kB\sin\theta)}{(kB\sin\theta)} \cos\theta \sin\phi \ , \tag{58}$$

$$E_\phi = i\eta_o I_o \left(\frac{kB}{2}\right) \frac{e^{ikR_o}}{R_o} J_1'(kB\sin\theta) \cos\phi \ . \tag{59}$$

With uniform current, a circular loop does not produce any θ-component of the electric field. Thus, the existence of E_θ in the present case is attributed to the non-uniform current carried by the loop.

3.4 Discussion

On the basis of Eqs. (58) and (59), we make the following comments with regard to the radiation field produced by a circular loop carrying a non-uniform current $I = I_o \cos\phi$:

(i) Near $\theta \sim 0^o$ the Bessel functions in (58) and (59) may be replaced by their small argument values i.e. $J'(x) \simeq 1/2$ and $J_1(x)/x \sim 1/2$. Thus the total far field may be written as

$$\vec{E} = \hat{\theta} E_\theta + \hat{\phi} E_\phi$$

$$\simeq i\eta_o I_o \left(\frac{kB}{2}\right) \frac{e^{ikR_o}}{R_o} \frac{1}{2} \left(\hat{\theta} \cos\theta \sin\phi + \hat{\phi} \cos\phi\right)$$

$$= i\eta_o I_o \left(\frac{kB}{2}\right) \frac{e^{ikR_o}}{R_o} \frac{1}{2} \hat{y} . \qquad (60)$$

Eq. (60) means that near the axial region of space ($\theta \sim 0^o$) the far electric field is not equal to zero and it is polarized along the y-direction.

(ii) In the $\phi = 0^o$ plane, i.e. in the vertical plane containing the directions of maxima of the figure-of-eight excitation, the field is polarized in the ϕ-direction and is given by:

$$E_\theta \equiv 0$$

$$E_\phi = i\eta_o I_o \left(\frac{kB}{2}\right) \frac{e^{ikR_o}}{R_o} J_1' (kB \sin\theta). \qquad (61)$$

(iii) In the $\phi = \frac{\pi}{2}$ plane i.e. in the vertical plane containing the directions of minima of the figure-of-eight excitation, the horizontal (i.e. ϕ-component) component of the electric field is identically equal to zero and the electric field is given by:

$$E_\theta = i\eta_o I_o \left(\frac{kB}{2}\right) \frac{e^{ikR_o}}{R_o} \frac{J_1(kB\sin\theta)}{(kB\sin\theta)} \cos\theta, \tag{62}$$

$$E_\phi \equiv 0$$

(iv) In the $\phi = \frac{\pi}{4}$ plane

$$E_\theta = i\eta_o I_o \left(\frac{kB}{2}\right) \frac{e^{ikR_o}}{R_o} \frac{J_1(kB\sin\theta)}{(kB\sin\theta)} \frac{\cos\theta}{\sqrt{2}}, \tag{63}$$

$$E_\phi = i\eta_o I_o \left(\frac{kB}{2}\right) \frac{e^{ikR_o}}{R_o} \frac{J_1'(kB\sin\theta)}{\sqrt{2}}. \tag{64}$$

(v) In the horizontal plane $\left(\theta = \frac{\pi}{2}\right)$,

$$E_\theta \equiv 0$$

$$E_\phi = i\eta_o I_o \left(\frac{kB}{2}\right) \frac{e^{ikR_o}}{R_o} J_1'(kB)\cos\phi. \tag{65}$$

The implications of the above comments will be investigated in the future in connection with the radiation field produced by a non-uniformly excited parasitic loop counterpoise antenna.

The results obtained can be used in the future to develop a theory for the radiation field produced by a non-uniformly excited parasitic loop counterpoise antenna. The important findings of the present investigation are that the non-uniformity of the current produces the following two effects: (i) the field is non-zero in the axial direction, and (ii) there exists a cross-polarized component of the field.

By assuming an excitation of the form given by Eq. (42) (which is the case with the standard VOR antenna) we have obtained theoretical expressions for the far field produced by a loop counterpoise antenna (no parasitic loops). Currently this expression is being programmed and the results will be reported later.

4. Experimental Investigation of Non-Uniformly Excited Double Parasitic Loop Counterpoise Antenna

Non-uniform excitation of the parasitic loop counterpoise antenna gives rise to some new phenomena not encountered in the uniformly excited cases. In general for the non-uniform case, the fields incident at the parasitic loops are different than in the uniform case. As a result of this the performance of the antenna is expected to be different than the latter. The non-uniform currents in the parasitic loops produce strong lobes in the axial directions. If they are found objectionable, their amplitudes can be considerably reduced by properly choosing the heights of the parasitic loops above the counterpoise. For example the axial lobe amplitude would be minimum if the height H of the parasitic loop satisfies the relation $H = n\,\lambda/2$ where n is an integer and λ is the wavelength. Since the nature of the excitation is different, it is also anticipated that the optimum parameters necessary for obtaining the best field gradient from the antenna would be different than those for the uniform case.

In view of the above, we have undertaken a systematic experimental investigation of the non-uniformly excited parasitic loop counterpoise antenna. The results reported below have been obtained from a 5.2' diameter counterpoise case and the measurements have been carried out in our indoor antenna pattern range. This was done because of bad weather conditions outside. The pattern characteristics have been measured at the frequency 1080 MHz (λ = 10.93"). The excitation used has been a pair of Alford loops spaced 3.2" apart and located at a height 4'8" above the counterpoise. The two loops are excited out of phase so that the combined field produced by them has a figure-of-eight variation in the azimuthal plane. All the parasitic loops

used have been fabricated from 1" wide conducting strips.

4.1 Preliminary Experiment

An initial radiation pattern investigation has been carried out for a double parasitic loop system with

$$H_2 = 22\frac{3}{8}'' \quad , \quad 2B_2 = 36'' \qquad \text{and} \qquad H_1, B_1 \text{ variable} ,$$

(see Fig. 1 for the notations). The purpose of this experiment has been to determine the effects of the parameters H_1, B_1 on the pattern and in particular to search for those values of H_1 and B_1 which may produce large field gradients at the horizon. The parameters H_2, B_2 were chosen on the basis of our previous investigation of single parasitic loop counterpoise antennas (Sengupta and Ferris, 1969).

The far field elevation patterns of the antenna have been measured at 1080 MHz with $2B_1$ varying in steps of 4" from 36" to 60" for each value of H_1. H_1 was varied from 4" to 7" in convenient steps. The main conclusion from this set of pattern results is that for low axial lobe and reasonably large field gradient $H_1 \sim 6''$ and $2B_1$ should lie between 48" - 60" . The important pattern characteristics obtained from this experiment are shown in Table 1. The different notations used in Table 1 are given below.

E_{max}	The amplitude of the far field in the direction of the principal maximum.
$E(\pi/2)$	Amplitude of the far field in the direction of the horizon i.e. $\theta = \pi/2$.
$E(96^o)$	Amplitude of the far field in the direction $\theta = 96^o$.
E_s	Amplitude of the first secondary lobe maximum below the horizon.
α_g	The field gradient/6^o at the horizon.
$E(0^o)$	Amplitude of the far field in the direction $\theta = 0^o$.
$E_s = E(\pi/2)$	Level of the secondary lobe maximum field relative to the field at the horizon.

All the above results are expressed in dB.

Table 1: Pattern Characteristics of a Non-Uniformly Excited Double Parasitic Loop Counterpoise Antenna. H_2= 22 3/8", $2B_2$=36", H_1=6", $2B_1$ variable.

$2B_1$	36"	40"	44"	48"	52"	56"	60"
E_{max}	-3.0	-5.5	-3.0	-3.0	-5.0	-5.0	-6.0
$E(\pi/2)$	-28.5	-22.0	-19.0	-25.0	-22.0	-22.0	-32.0
$E(96^o)$	-35.0	-25.5	-28.0	-35.0	-29.0	-33.0	<-40.0
E_s	-27.0	---	-32.0	-28.0	---	-35.0	-33.0
$E(0^o)$	-22.0	-17.0	-16.0	-19.0	-19.0	-25.0	-23.0
α_g	6.5	3.5	9.0	10.0	7.0	11.0	> 8.0
E_s-$E(\pi/2)$	1.5	---	-13.0	-3.0	---	-13.0	-1.0

The values that are left out in the above table were found to be not applicable to the measured patterns. Three complete patterns are shown in Figs. 5a — 5c for three selected cases.

4.2 Optimization of the Lower Parasitic Loop Parameters

The next set of data have been taken for the purpose of obtaining the best values of the lower parasitic loop parameters H_1, B_1 for some fixed values H_2, B_2 of the upper parasitic loop parameters. During this experiment the upper loop parameters were fixed at H_2= 22 3/8", $2B_2$= 36" . The diameter of the lower parasitic loops were varied from 54" - 60" in steps of 2" . For each value of $2B_1$, H_1 was varied from 5" - 7" in some convenient steps. The various pattern characteristics as obtained from the measured elevation patterns are shown in Tables 2, 3, and 4.

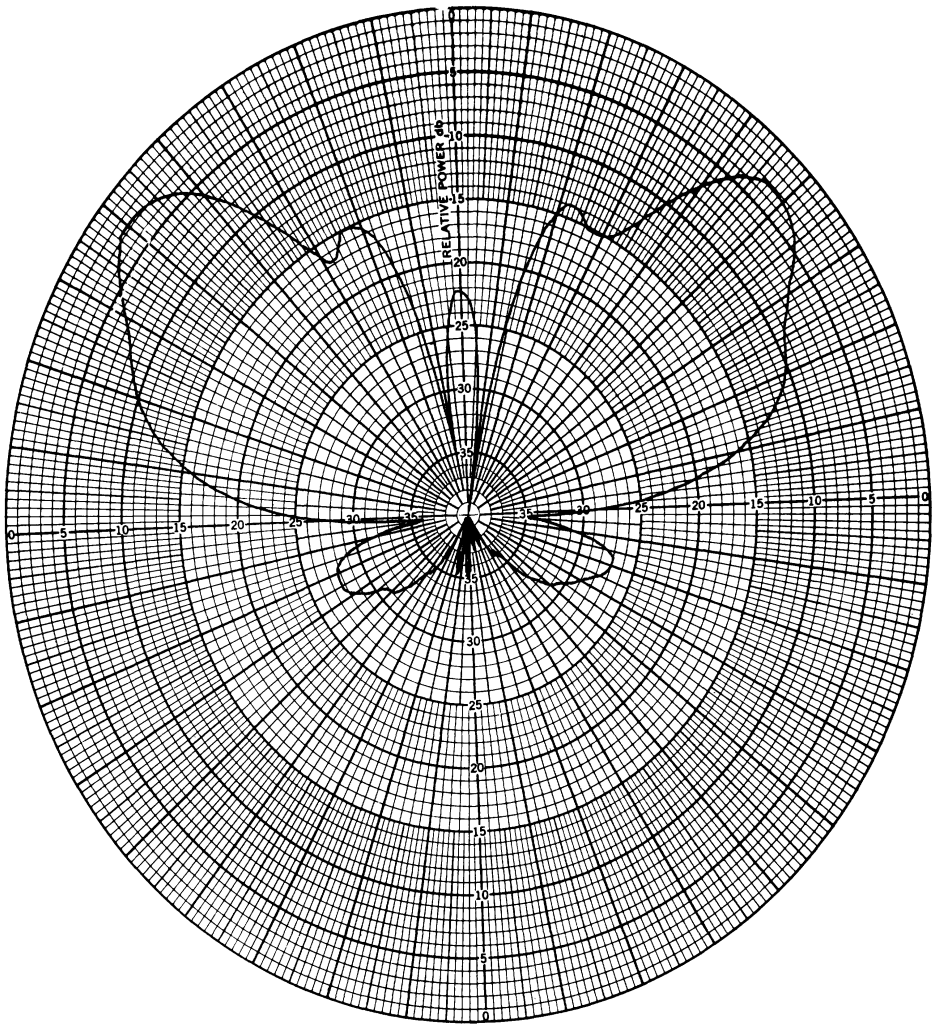

FIG. 5a: Measured Elevation Patterns of a Double Parasitic Loop Counterpoise Antenna. 2A=5.2', h=4.8", f=1080 MHz, $2B_2$=36", H_2= 22 3/8", H_1=6" and $2B_1$=36" .

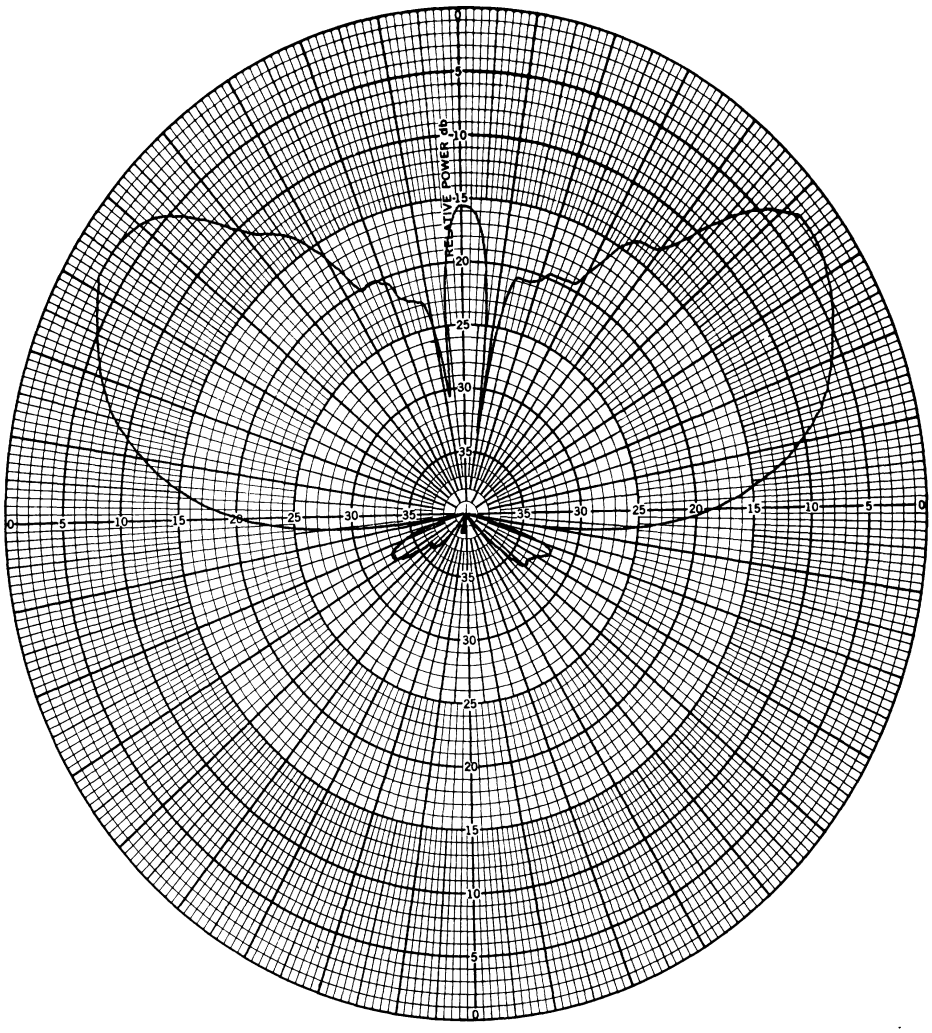

FIG. 5b: Measured Elevation Patterns of a Double Parasitic Loop Counterpoise Antenna. 2A=5.2', h=4.8", f=1080 MHz, $2B_2$=36", H_2= 22 3/8", H_1=6" and $2B_1$ = 44 .

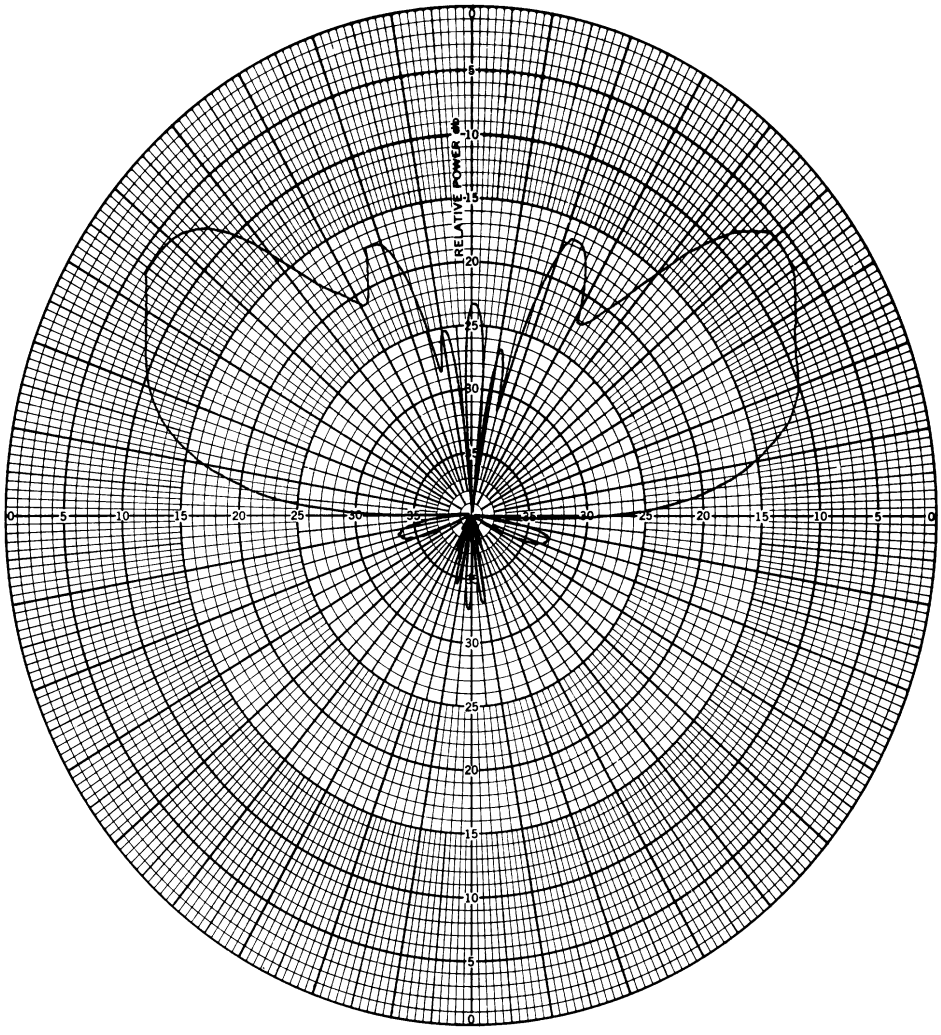

FIG. 5c: Measured Elevation Patterns of a Double Parasitic Loop Counterpoise Antenna. 2A=5.2', h=4.8", f=1080 MHz, $2B_2$=36", H_2= 22 3/8; H_1=6" and $2B_1$= 60" .

Table 2: Pattern Characteristics of a Non-Uniformly Excited Double Parasitic Loop Counterpoise Antenna. $2B_2$=36", H_2= 22 3/8", $2B_1$=54", H_1 variable.

H_1	5 1/2"	5 3/4"	6"
E_{max}	-7.0	-7.0	-7.0
$E(\pi/2)$	-22.0	-23.0	-23.0
$E(96^o)$	-28.0	-30.0	-32.0
E_s	---	---	---
$E(0^o)$	-27.0	-28.0	-22.0
α_g	6.0	7.0	9.0

Table 3: Pattern Characteristics of a Non-Uniformly Excited Double Parasitic Loop Counterpoise Antenna. $2B_2$=36", H_2=22 3/8", $2B_1$=56", H_1 variable.

H_1	5"	5 1/2"	5 3/4"	6"	6 1/4"	7"
E_{max}	-5.0	-5.0	-5.0	-5.0	-5.0	-5.0
$E(\pi/2)$	-20.0	-21.0	-22.5	-23.0	-24.0	-26.0
$E(96^o)$	-26.5	-30.0	-32.0	-32.0	-33.0	-35.0
E_s	-37.0	---	---	-36.0	-33.5	-31.0
$E(0^o)$	-22.0	-30.0	-30.0	-24.0	-20.0	-15.0
α_g	6.5	9.0	9.5	9.0	9.0	10.0
E_s-$E(\pi/2)$	-17.0	---	---	-13.0	-9.5	-5.0

Table 4: Pattern Characteristics of a Non-Uniformly Excited Double Parasitic Loop Counterpoise Antenna. $2B_2$=36", H_2= 22 3/8", $2B_1$=58", H_1 variable.

H_1	5 1/2"	5 3/4"	6"
E_{max}	-6.0	-6.0	-6.0
$E(\pi/2)$	-24.0	-25.0	-26.0
$E(96^o)$	-35.0	-35.0	-35.0
E_s	-36.0	-36.0	-35.0
$E(0^o)$	-28.5	-29.0	-26.5
α_g	11.0	10.0	9.0
E_s-$E(\pi/2)$	-12.0	-11.0	-9.0

From the previous tables it is found that for values of the parameter H_1 between 5 1/2" and 5 3/4" the lobe maximum in the direction $\theta=0^o$ is minimum. Notice that theoretically, for minimum axial lobe $H_1 = \lambda/2 = 5.465"$ at f=1080 MHz.

From the results given in this section, it appears that the best pattern for possible VOR application is obtained when $2B_2 = 36"$, $H_2 = 22\ 3/8"$, $2B_1 = 56"$ and $H_1 = 5\ 3/4"$. The measured elevation pattern for this case is shown in Fig. 6.

4.3 Optimization of the Upper Parasitic Loop Parameters

In this set of experiments the lower parasitic loop parameters were fixed at $2B_1=56"$ and $H_1=5\ 3/4"$. The height of the upper loop was fixed at the value $H_2 = 22\ 3/8"$ while the diameter $2B_2$ was varied from 34" — 40" . The results are shown in Table 5. Note that the field gradient values shown in Table 5 have been obtained from the measured polar plots and hence are approximate. More accurate values for α_g in some specific cases will be discussed in the next paragraph.

Table 5: Pattern Characteristics of a Non-Uniformly Excited Double Parasitic Loop Counterpoise Antenna.
$2B_1=56"$, $H_1=5\ 3/4"$, $H_2 = 22\ 3/8"$, $2B_2$ variable.

$2B_2$	34"	35"	36"	37"	38"	39"	40"
E_{max}	-5.0	-5.0	-6.0	-6.0	-6.0	-5.0	-5.0
$E(\pi/2)$	-19.5	-20.5	-21.0	-22.5	-24.0	-25. 5	-24.5
$E(96^o)$	-26.5	-28.0	-29.5	-32.0	-35.5	-36.0	-34.0
E_s	---	---	---	-36.0	-34.0	-32.0	-31.0
$E(0^o)$	-27.0	-28.0	-28.0	-29.0	-35.0	-35.0	-35.0
α_g	7.0	7.5	8.5	9.5	11.5	11.5	9.5
$E_s - E(\pi/2)$	---	---	---	-13.5	-10.0	-10.0	-6.5

A typical measured pattern having desirable characteristics is shown in Fig. 7.

To obtain more accurate estimates for the field gradients, rectangular plots for the patterns have been obtained in ordinary and expanded scales for some selected cases. The patterns obtained in a few interesting cases are shown in Figues 8, 9a - 9b, and 10a - 10b . As can be seen from these figures a field gradient value better than 12 dB can be obtained without appreciably increasing the field in the axial direction.

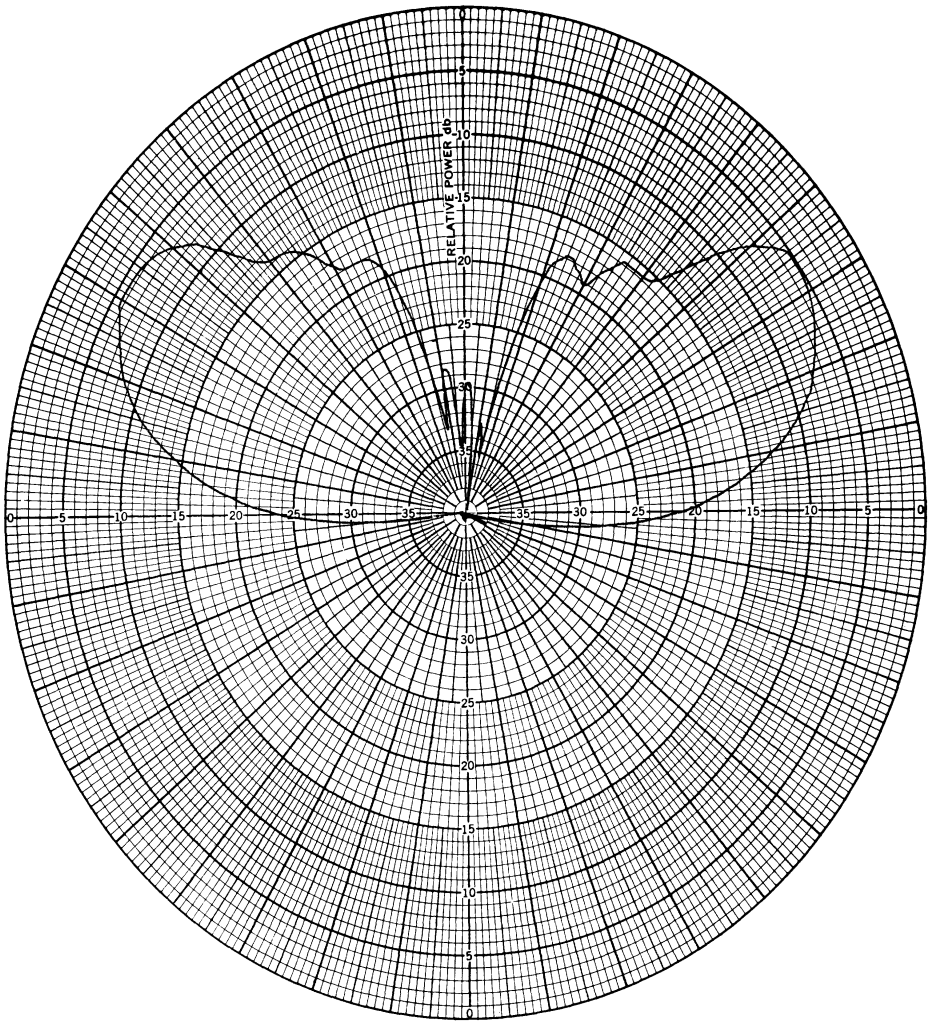

FIG. 6: Measured Elevation Pattern of a Double Parasitic Loop Counterpoise Antenna. 2A=5.21, h=4.8", $2B_1$=56", H_1= 5 3/4", $2B_2$=36", H_2= 22 3/8", f = 1080 MHz.

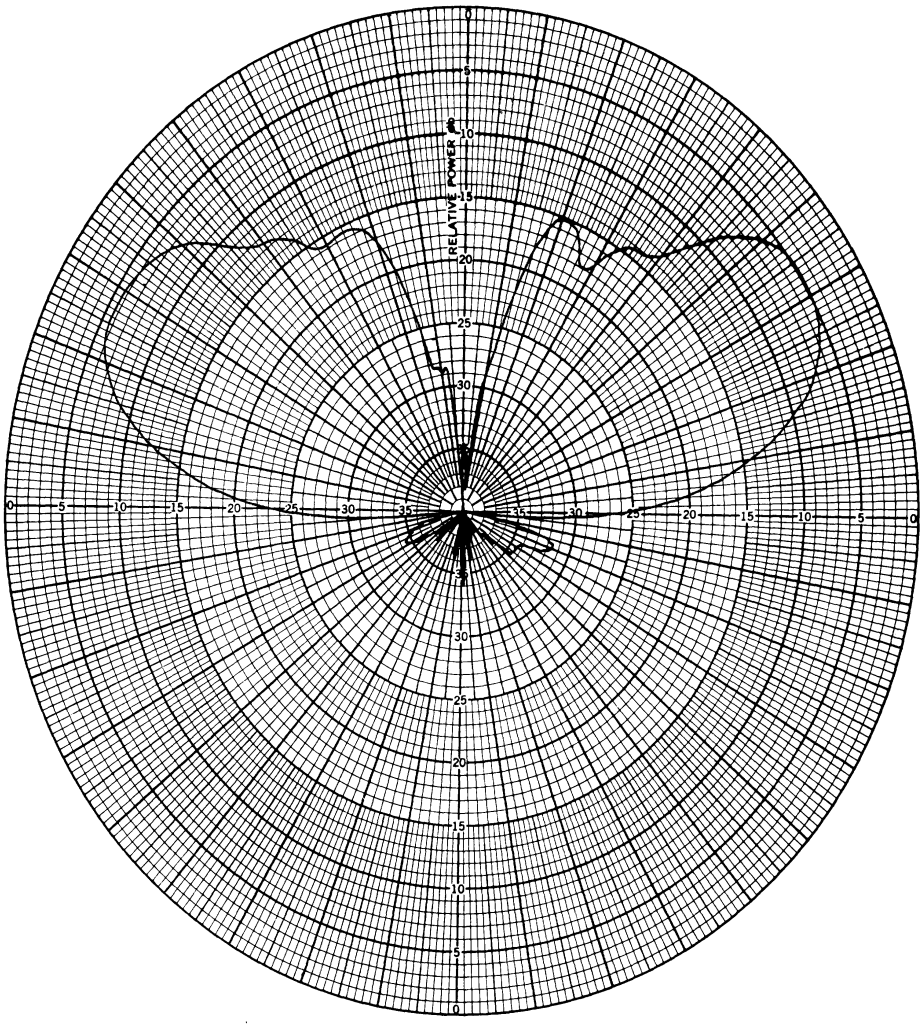

FIG. 7: Measured Elevation Pattern of a Double Parasitic Loop Counterpoise Antenna. 2A=5.2', h=4.8", $2B_1$=56", H_1= 5 3/4", $2B_2$= 40", H_2= 22 3/8", f = 1080 MHz.

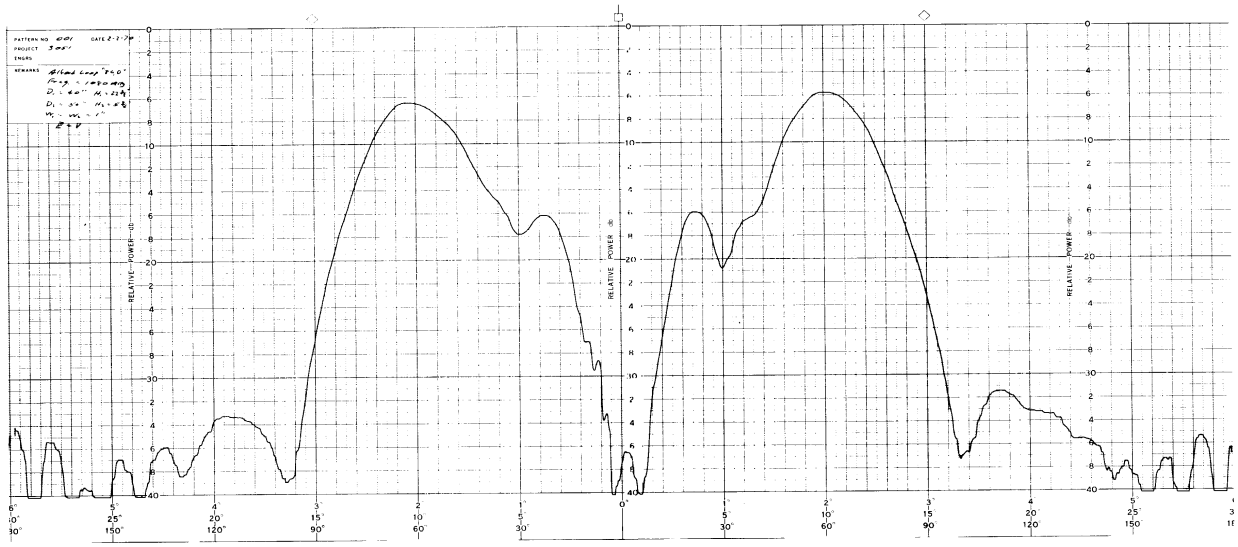

FIG. 8: Measured Elevation Pattern of a Double Parasitic Loop Counterpoise Antenna. 2A=5.2', h=4.8", $2B_1$=56", H_1= 5 3/4", $2B_2$= 40", H_2= 22 3/8", f = 1080 MHz.

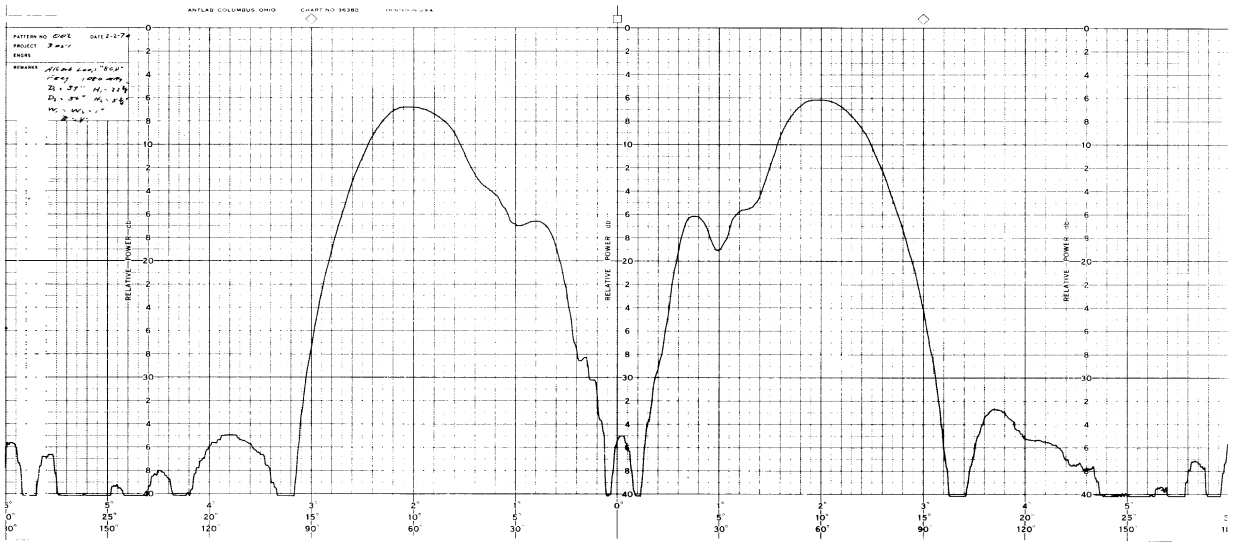

FIG. 9a: Measured Elevation Pattern of a Double Parasitic Loop Counterpoise Antenna - Complete Pattern. 2A=5.2', h=4.8", $2B_1$=56", H_1= 5 3/4", $2B_2$= 39", H_2= 22 3/8", f = 1080 MHz.

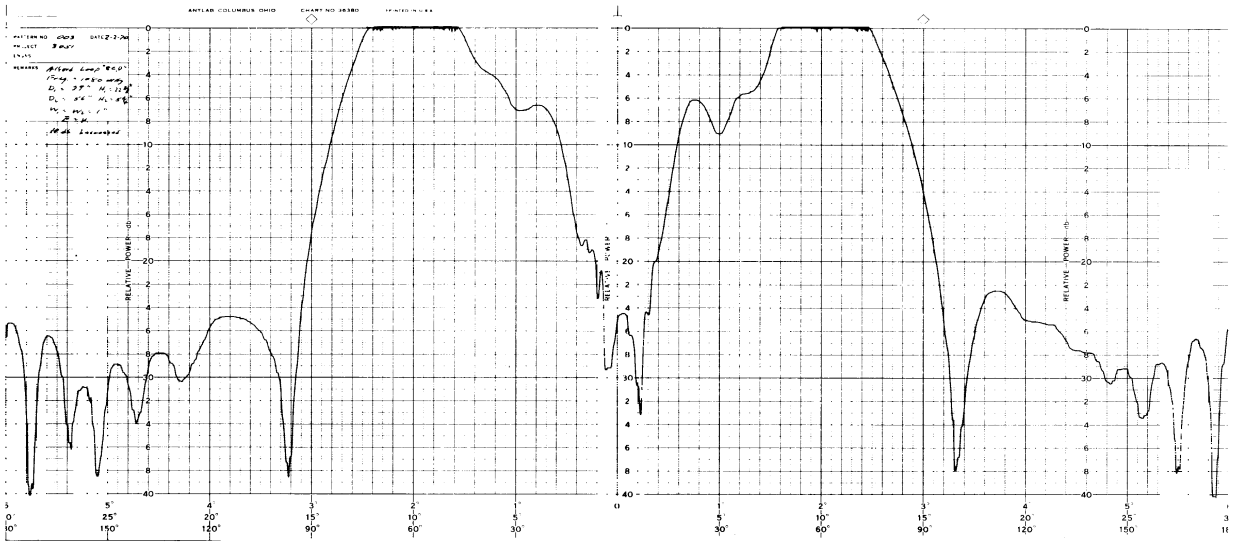

FIG. 9b: Measured Elevation Pattern of a Double Parasitic Loop Counterpoise Antenna - Details Near and Below the Horizon. 2A=5.2', h=4.8", $2B_1$=56", H_1=5 3/4", $2B_2$=39", H_2= 22 3/8", f = 1080 MHz.

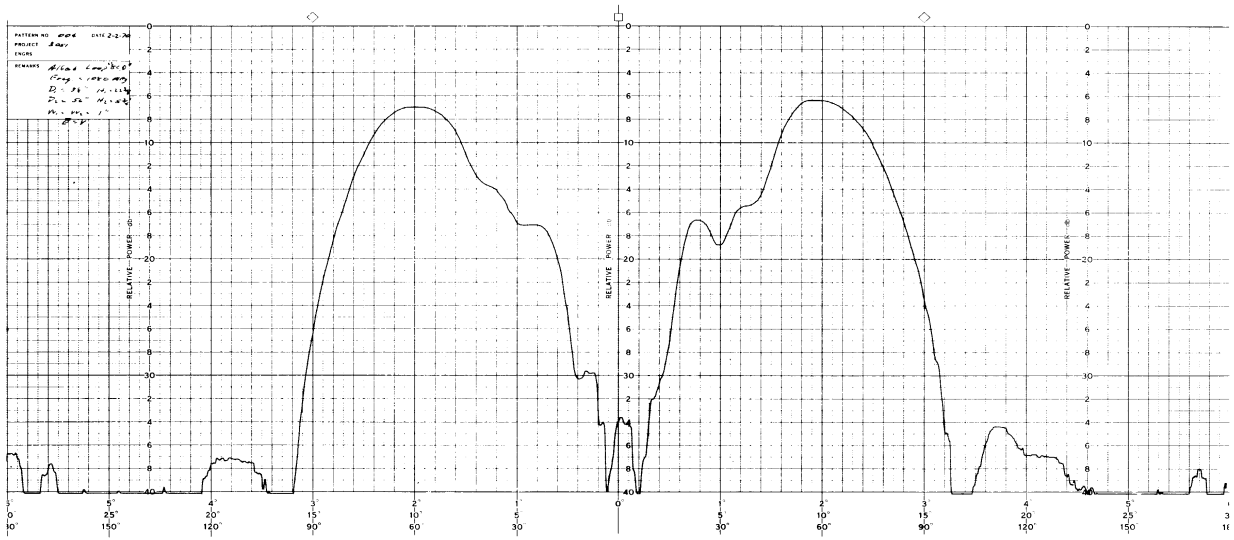

FIG. 10a: Measured Elevation Pattern of a Double Parasitic Loop Counterpoise Antenna - Complete Pattern. 2A=5.2', h=4.8", $2B_1$=56", H_1=5 3/4", $2B_2$= 38", H_2== 22 3/8, f=1080 MHz.

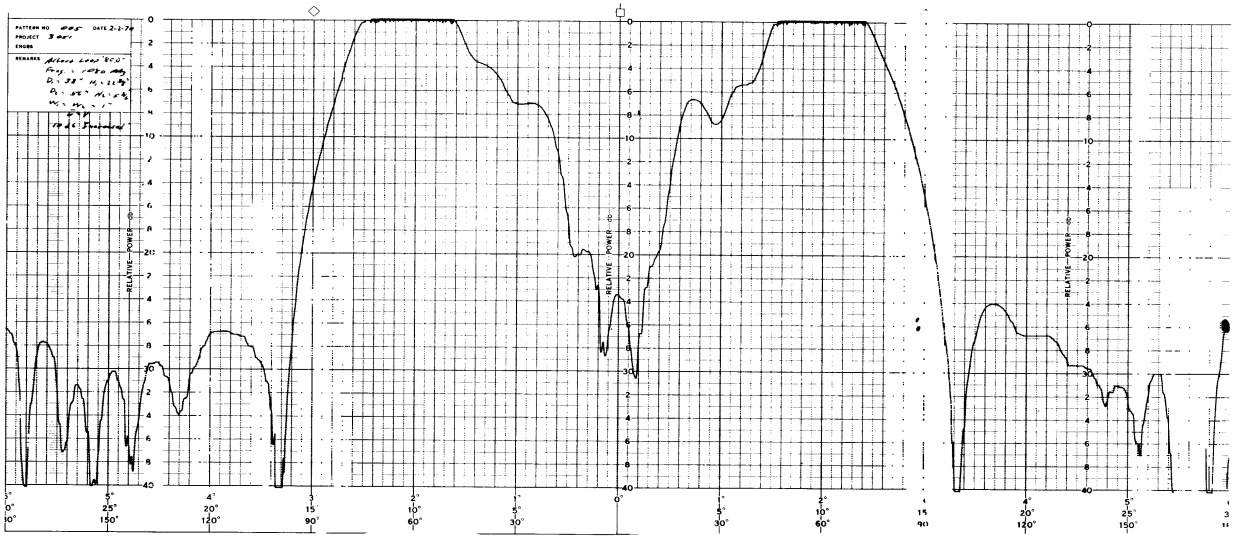

FIG. 10b: Measured Elevation Pattern of a Double Parasitic Loop Counterpoise Antenna - Details Near and Below the Horizon. 2A=5.2', h=4.8", $2B_1$=56", H_1=5 3/4", $2B_2$=38", H_2=22 3/8", f = 1080 MHz.

4.4 Maximum Obtainable Field Gradient

Two main criteria governed the basis of the investigations discussed in the preceding sections. These are (i) the field gradient at the horizon be high, and (ii) the axial lobe amplitude be as small as possible. In this section we give the results obtained from an experiment where the second restriction on the pattern has been removed. The aim of this part of the investigation has been to determine the largest value of the field gradient that can be obtained from a double parasitic loop counterpoise antenna. The results are shown in Figs. 11a and 11b . In this particular case the field gradient at the horizon is found to be better than 22 dB/6^{o} which may be considered to be a dramatic improvement.

5. Discussion

The above results represent the present status of the theoretical and experimental investigation of the radiation characteristics of non-uniformly excited parasitic loop counterpoise antennas. The experiments results for the 5.2' diameter counterpoise case are almost complete. Development of the theoretical expressions for the radiation field and their numerical evaluation will be done during the coming period.

6. Conclusion

On the basis of the results given above it can be concluded that the parasitic loop concept has been found to be highly effective in improving the field gradient characteristics of a non-uniformly excited parasitic loop counterpoise antenna. From our investigation of the radiation characteristics of a double parasitic loop counterpoise antenna having figure-of-eight type of excitation we make the following two important observations.

(i) It is possible to obtain a field gradiant at the horizon better than 12 dB/6^{o} while maintaining the field in the axial direction to be less than 25 dB down from the field in the principal maximum direction.

(ii) It is possible to obtain a field gradient at the horizon better than 22 dB/6^{o} while maintaining the axial field to be less than 16 dB down from the field in the

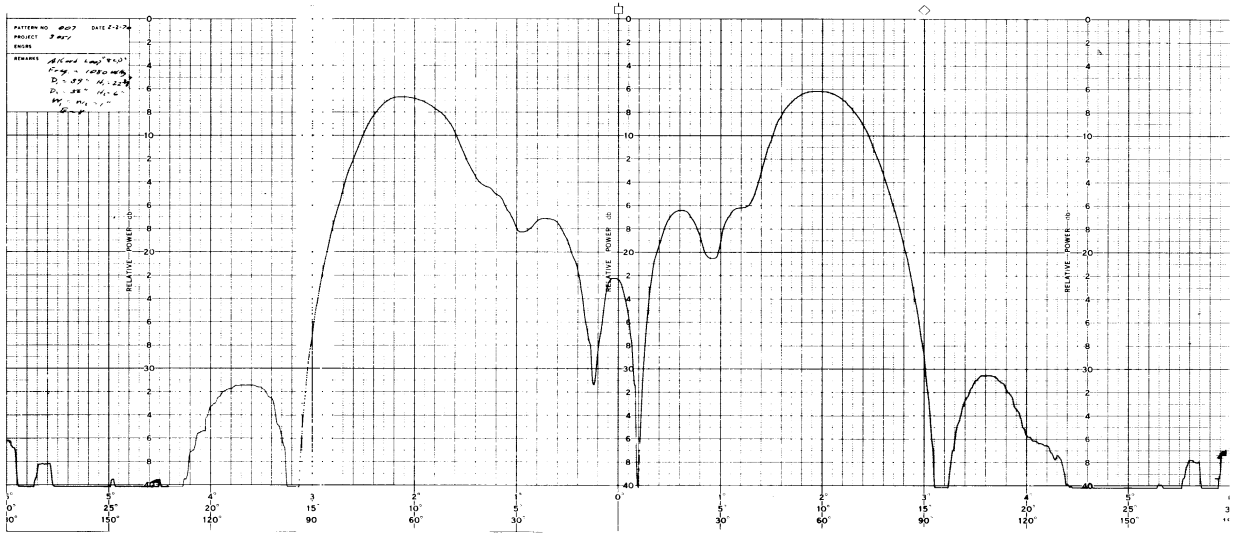

FIG. 11a: Measured Elevation Pattern of a Very Large Gradient Double Parasitic Loop Counterpoise Antenna - Complete Pattern. $2A=5.2'$, $h=4.8''$, $2B_1=56''$, $H_1=6''$, $2B_2=39''$, $H_2=22\ 3/8''$, $f=1080MHz$.

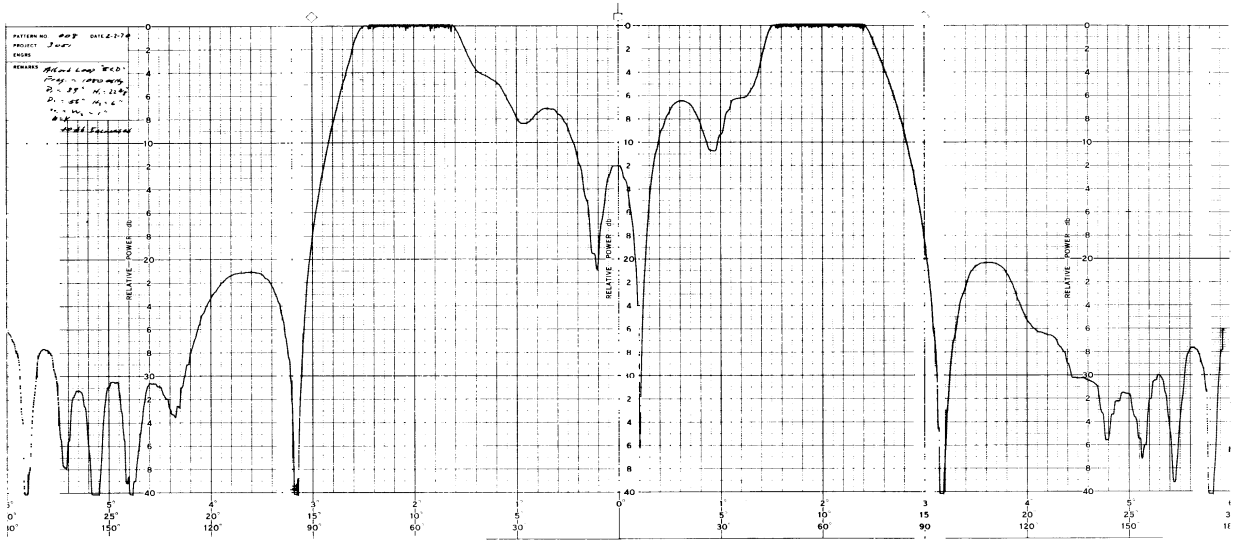

FIG. 11b: **Measured Elevation Pattern of a Very Large Gradient Double Parasitic Loop Counterpoise Antenna - Details Near and Below the Horizon. 2A=5.2', h=4.8", $2B_1$=56", H_1=6", $2B_2$=39", H_2=22 3/8", f=1080 MHz.**

principal maximum direction.

In all the above cases the secondary lobe maximum below the horizon has been found to be about 9 - 12 dB down from the field at the horizon.

7. References

Sengupta, D. L., J. E. Ferris and V. H. Weston (1968), "Theoretical and Experimental Investigation of Parasitic Loop Counterpoise Antennas - Final Report," The University of Michigan Radiation Laboratory Report 8905-1-5, FAA Report No. SRDS, RD-68-50.

Sengupta, D. L., and J. E. Ferris (1969), "VOR Parasitic Loop Counterpoise System-II," Interim Report No. 1, The University of Michigan Radiation Laboratory Report 3051-1-T.

Sengupta, D. L. and V. H. Weston (1969), "Investigation of the Parasitic Loop Counterpoise Antenna," IEEE Trans., AP-17, No. 2, pp. 180-191.